



Mass distribution and concentrations of negative chemiions in the exhaust of a jet engine: Sulfuric acid concentrations and observation of particle growth

Thomas M. Miller^a, John O. Ballenthin^a, A.A. Viggiano^{a,*},
Bruce E. Anderson^b, Chowen C. Wey^c

^a*Air Force Research Laboratory, Space Vehicles Directorate, Hanscom Air Force Base, 29 Randolph Road, Hanscom AFB, MA 01731-3010, USA*

^b*Atmospheric Sciences Division, National Aeronautics and Space Administration, Langley Research Center, Hampton, VA 23681-0001, USA*

^c*Engine Components Division, Army Research Laboratory/High Speed Systems Office, National Aeronautics and Space Administration, Glenn Research Center, Cleveland, OH 44135, USA*

Received 10 July 2004; accepted 11 January 2005

Abstract

Measurements of negative-ion composition and density have been made in the exhaust of a J85-GE-5H turbojet, at ground level, as part of the NASA-EXCAVATE campaign. The mass spectrometer was placed 3 m from the exhaust plane of the engine. Measurements were done as a function of engine power in six steps from idle (50%) to military power (100%). Since the exhaust velocity changes with power, this also corresponds to a time evolution for ion growth. At 100% power most of the ions are HSO_4^- with minor amounts of $\text{HSO}_4^-(\text{H}_2\text{O})_n$. With decreasing engine power the degree of hydration increases. In addition, ions with a 139-amu core dominate the spectra at lower engine power. The chemical identity of this ion is unknown. Observation of a small amount of NO_3^- core ions in the high-power spectra allows the determination of H_2SO_4 concentrations, which turn out to be a fraction-of-a-percent of the total sulfur in the fuel. Combining the present data with several previous composition measurements allows one to observe ion evolution from bare ions to ions with masses >8000 amu. Ion densities are derived and appear consistent with previous measurements used in modeling studies indicating that ion nucleation is a probable mechanism for volatile aerosol formation.

Published by Elsevier Ltd.

Keywords: Jet engine; Ion-induced nucleation; Aerosol growth; Sulfuric acid; Mass spectrometer

1. Introduction

Chemiions produced in jet engine combustion are speculated to play a role in ion-induced nucleation of aerosols, possibly followed by condensation, which may result in the formation of contrails, cirrus clouds, and pollutants (Arnold et al., 1996; Eichkorn et al., 2002;

*Corresponding author. Tel.: +1 781 377 4028; fax: +1 781 377 1148.

E-mail address: albert.viggiano@hanscom.af.mil (A.A. Viggiano).

Frenzel and Arnold, 1994; Haverkamp et al., 2004; Kärcher et al., 1998; Kiendler and Arnold, 2002a,b; Lovejoy et al., 2004; Sorokin et al., 2003; Wohlfrom et al., 2000; Yu and Turco, 1998, 1999; Yu et al., 1999). The main argument against this notion is that aerosol concentrations tend to be orders of magnitude greater than the estimated ion concentrations. However, it is possible that ion-induced nucleation will be found to be the source of a particular type of aerosol or a particular size range. No direct connection has yet been demonstrated, though Arnold and colleagues have reported observation of massive positive and negative chemions (Eichkorn et al., 2002; Haverkamp et al., 2004; Wohlfrom et al., 2000). That group has performed a number of pioneering experiments to identify the ion types and concentrations emitted by jet engines, both at ground level (Arnold et al., 1998; Kiendler et al., 2000; Kiendler and Arnold, 2002b) and in flight (Arnold et al., 1999; Wohlfrom et al., 2000). These studies showed plasma densities at the exhaust plane of various jet engines to be in the 10^9 cm^{-3} range. However, a common feature of all these measurements are relatively large times (hundreds of ms) spent in sampling. A new measurement using an ion mobility spectrometer that obtained ion distributions (without resolved masses) at 2 ms after the combustor is an exception (Haverkamp et al., 2004).

There exists a natural limitation to the buildup of very large plasma densities in the combustion plume, namely positive-ion/negative-ion recombination (Arnold, 1980; Bates, 1982, 1985; Smith and Adams, 1982), a process involving electron transfer from a negative ion to a positive ion during an interaction. Effective neutralization may occur when two ions coalesce even if the electron binding energy of the negative ion has been increased, via stabilization by adducts, beyond the electron capture energy of the positive ion (Arnold, 1980; Moseley et al., 1975; Turco et al., 1998). If the applicable ternary ion-ion recombination rate constant is known, it may be used to estimate the ion concentration from the combustor through to the exhaust wake.

Another interesting question that ion composition measurements can address is the amount of sulfuric acid in the exhaust plume (Arnold et al., 1996; Curtius et al., 1998; Frenzel and Arnold, 1994). In the engine, fuel sulfur is oxidized to form SO_2 . In the engine or exhaust, the SO_2 reacts with OH to form HSO_3 , which quickly converts to SO_3 . As the gases cool, the SO_3 is converted to H_2SO_4 in a reaction that involves two H_2O molecules (Jayne et al., 1997; Kolb et al., 1994; Lovejoy et al., 1996; Reiner and Arnold, 1994). The most sensitive detection method for H_2SO_4 concentrations is ion chemistry, in particular the conversion of NO_3^- core ions into HSO_4^- core ions (Viggiano et al., 1980, 1982, 1997). This method has been used in engine exhaust as well as the ambient atmosphere (Arnold et al., 1981;

Eisele and Tanner, 1993; Viggiano and Arnold, 1983). This method works since NO_3^- is rapidly produced in atmospheric plasmas containing even trace amount of NO_x species (Ferguson et al., 1979; Viggiano and Arnold, 1995). Ions with this core are very stable, with the only reactivity being proton transfer from species having larger gas phase acidities than HNO_3 , H_2SO_4 being the most prominent (Viggiano et al., 1992).

2. The J85-GE-5H turbojet engine

The J85-GE-5H augmented turbojet engine was one of the two on a NASA T-38 Talon aircraft. This type of engine has been in service since 1960 and has a high thrust-to-weight ratio. It has eight stages of compression and two turbine stages. It is in the 12-kN thrust range. The T-38 was parked on a run-up area of the tarmac at NASA-Langley Research Center (LaRC) for the measurements described here. The engine was operated with JP-5 fuel which contained 810 parts per million by mass (ppmm) sulfur. The engine has an augmenter (afterburner) section which places the exhaust plane of the engine further from the combustors than in a normal commercial jet engine. In these tests, the engine was operated at six different compressor rpm, where 100% denotes the maximum rpm, or “military power”. The relation between thrust and rpm is linear enough that the terms “70% maximum rpm” and “70% power” may be considered equivalent.

3. Experimental

The AFRL ion mass spectrometer (IMS) was mounted onto a stainless-steel sampling pipe, as shown in Fig. 1. The sampling orifice of the IMS protruded into the exhaust sampling pipe by 0.4 cm. Chemions entrained in exhaust gases thus entered the first stage of differential pumping. An electric potential on a skimmer pulled ions into the high-vacuum region

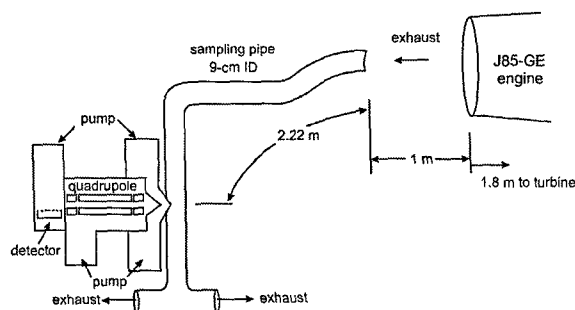


Fig. 1. A sketch of the sampling arrangement for the IMS behind the J85-GE jet engine.

containing an RF electric quadrupole mass analyzer with RF-only focusing rods on both the entrance and exit. The mass analyzed ions were detected with a discrete-dynode electron multiplier. The mass spectrometer system has been described in detail in earlier publications, where it was used as a chemical ionization detector of trace neutrals (Ballenthin et al., 2003; Hunton et al., 2000; Miller et al., 2000). Here the ions are formed in the engine instead of the corona source. The IMS was encased in a blast shield which was below the level of the jet engine. The RF resonator of the mass spectrometer gave a mass range of 745 amu in the present work.

In mass resolving mode, the quadrupole mass analyzer utilized RF and DC potentials in order to give stable trajectories to ions of a selected q/m . If the quadrupole was operated with only RF potentials, the device acted as a very broad filter with masses from 9/7 to 16 times the resolving mass passed. For most purposes this can be considered as a high-pass filter and we will refer to these data as integral-mode spectra. Comparison with the mass-resolved intensities allows one to judge the transmission efficiency. Comparison of the maximum and points along the total-ion curve allows one to deduce what fraction of the ions are beyond any given mass, and in particular, beyond the mass range of the instrument. In figures and tables where we deduce mass distributions based on the integral mass spectra (RF-only mode), the 9/7 factor was accounted for, i.e., the spectrum was scaled so that any breaks in the curve occurred at the appropriate ion mass.

In order to relate the detected ion intensities to the plasma density in the sampling pipe, laboratory calibrations of the total-ion detection efficiency ϵ of the IMS were carried out. A cylindrical Gerdien condenser was placed in the laboratory version of the sampling pipe, 7 cm from the IMS sampling orifice, and ions were generated with a corona source another 50 cm upstream of the Gerdien condenser. Partly because of ion-ion recombination, the maximum ion density that could be created in the laboratory flow tube was $4.8 \times 10^6 \text{ cm}^{-3}$ at 300 K. This low value of the maximum ion density was due to a relatively low bulk flow velocity of 10 m s^{-1} , compared to the flow velocity in the field ($60\text{--}400 \text{ m s}^{-1}$). Measurements of ϵ were made from 50 to 723 Torr. At the higher pressures, ϵ reached a constant value of $0.00102 \text{ cm}^3 \text{ counts s}^{-1}$, i.e., each ion count per second represented an ion concentration outside the sampling orifice of 980 cm^{-3} . Since it is the neutral gas flow through the orifice that sweeps ions into the mass spectrometer, it is straightforward to correct for the effect of temperature. For example, a flow calculator indicated that the gas flow through the orifice was 13% lower at 400 K than at 300 K. The calibration factor ϵ has been observed to be constant within 10% over a

Table 1
Pertinent operating parameters for the measurements behind a J85-GE-5H jet engine for various engine power levels

Engine power (%)	T (K), 1 m behind engine	Time (ms) from engine exhaust plane to IMS
100	693	8
90	613	10
80	583	16
70	573	25
60	348	39
50 (idle)	663	51

year's time. We estimate that the overall uncertainty in ϵ is 25%.

An attempt to use the Gerdien in the field tests, for a direct measurement of the ion density at 1 m behind the engine exhaust plane, failed due to an oil coating laid down at engine startup, a problem that could be solved in the future.

The sampling pipe was allowed to come into equilibrium with the engine exhaust and became hot. Table 1 gives the temperatures at the exit plane and 1 m downstream as well as the time from the exit plane to the mass spectrometer orifice. The minimum in temperature is related to the amount of bypass air that enters the exhaust. The temperature at the entrance to the mass spectrometer was not measured.

4. Results

Both mass spectra and integral-mode spectra were obtained with the J85-GE-5 engine operated at 100%, 90%, 80%, 70%, 60%, and 50% (idle) of maximum compressor (or turbine) rpm, with JP-5 fuel containing 810 ppm sulfur. The series from high to low power are related to the ion growth issue since the reaction time—from engine exhaust plane to IMS orifice—increases. However, there is not an exact correlation since temperature and other engine conditions also change. The mass resolving-mode data are shown in Fig. 2 for engine power from military power down to idle. Note that the y -axes cover several orders of magnitude of ion intensity. In Fig. 2(a), for 100% power, the spectrum is dominated by the HSO_4^- peak at 97 amu. The first and second hydrates of this ion are clearly observed, although in lower abundance. For example, the HSO_4^- peak in Fig. 2(a) is almost four times more intense than the first hydrate, and is 32 times more intense than the second hydrate. A small amount of NO_3^- and its first hydrate were observed, and is significant as NO_3^- is the presumed precursor to HSO_4^- . The only other

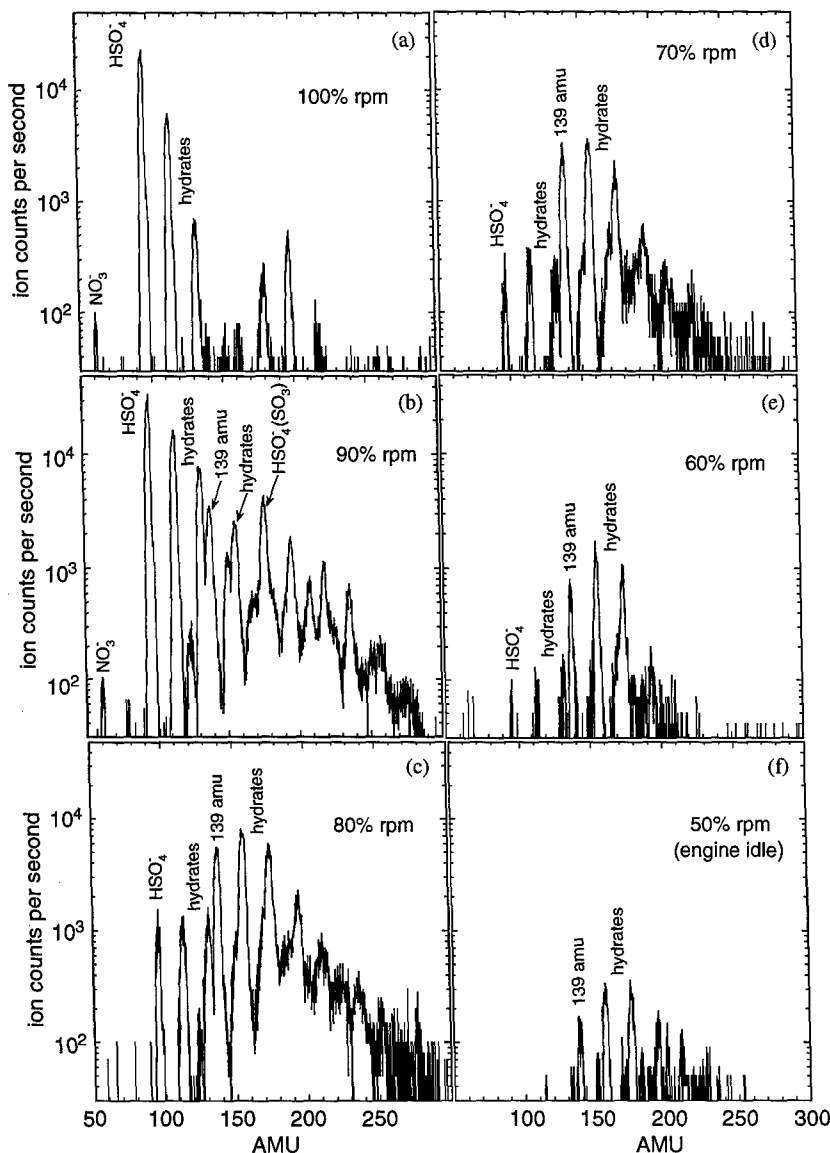


Fig. 2. Resolving-mode mass spectra at 1 m behind the J-85 jet engine.

appreciable peaks are at ~ 181 and 198 amu, the identities of which are not apparent.

Fig. 2(b) shows the mass spectrum for 90% power. HSO_4^- is still the dominant ion but is considerably more hydrated, with at least three and perhaps four hydrates being evident. The increased hydration is a result of a lower exhaust temperature than in 100%-power spectra—by 80 K at 1 m downstream. NO_3^- and its first hydrate are again observed in very small abundance. The small abundance (relative to the total-ion intensity) is due in part to the increased reaction time, since NO_3^- core ions react with H_2SO_4 (Viggiano et al., 1982, 1997). Also observed is $\text{NO}_3^-(\text{HNO}_3)$, which indicates that the gas has cooled enough so that HNO_3 can form by

recombination of OH with NO_2 . An ion at 139 amu is present at a level of 10% of the HSO_4^- signal, and its hydrate is almost as abundant. Many possible species containing only H, N, O, S, and C atoms exist as candidates to explain the 139-amu feature, but none stand out as being jet-fuel related. Several small, unresolved mass peaks were also observed. Clusters of the 139-amu ion with SO_3 and H_2SO_4 are also observed, with the SO_3 cluster being the larger of the two. This indicates that not all the SO_3 has converted to H_2SO_4 at this stage of ion evolution.

The mass spectrum obtained at 80% power is given in Fig. 2(c). The trend to more massive ions and greater hydration is clear. The $\text{HSO}_4^-(\text{H}_2\text{O})_n$ series is no longer

dominant and $n = 0, 1$, and 2 in this series are approximately equally abundant. As before, the additional hydration stems from the fact that the exhaust gas is cooler than in the higher-power spectra. This mass series is about an order of magnitude smaller than the series of ions with 139-amu cores. For the 139-amu series, the bare ion and the second hydrate are slightly less intense than the first hydrate, but all are roughly equal, indicating that the bond strengths are about the same as those in $\text{HSO}_4^-(\text{H}_2\text{O})_n$. The third hydrate of the 139-amu ion is a factor of three less abundant, again in indication of the temperature dropping with power. Any $\text{HSO}_4^-(\text{SO}_3)$ or $\text{HSO}_4^-(\text{H}_2\text{SO}_4)$ ions are masked by the hydrates of 139. No $\text{NO}_3^-(\text{H}_2\text{O})_n$ ions are observed but a small $\text{NO}_3^-(\text{HNO}_3)$ peak was observed. The rest of the peaks is small, broad, and blend into one another.

The 70%, 60%, and 50% (idle) spectra, Fig. 2(d–f), are reduced in intensity from the higher-power spectra. The reduction is not only due to lower ion production in the engine, but is also a result of the longer reaction time, during which a greater variety of more massive ions are produced, and losses occur to ion–ion recombination. The idle spectrum has a particularly low intensity. Two main series of ions are observed in each of these spectra, namely $\text{HSO}_4^-(\text{H}_2\text{O})_n$ and $139^-(\text{H}_2\text{O})_n$ with $n = 0–4$. The low-intensity ion at 194 ± 1 amu may be a hydrate of 139^- at 193 amu or may be $\text{HSO}_4^-(\text{H}_2\text{SO}_4)$ at 195 amu. The low intensity has made it impossible to determine which one or if both of these ions are present. The hydration sequences are similar to those found in the 80% spectrum although the exhaust temperature has increased.

We have not been able to find a likely candidate for the ion at 139 amu, which along with its hydrates dominates the lower-power spectra. The evolution of the spectra from high to low power indicates that ions with HSO_4^- cores react with trace gas to form the 139-amu core ions. However, HSO_4^- is very non-reactive since it has a high electron detachment energy (4.75 ± 0.10 eV) (Wang et al., 2000) and it is the base of a very strong acid (Viggiano et al., 1992). We searched the NIST WebBook (Mallard and Linstrom, 2001) for a neutral with a high electron affinity and a weight of 139 amu or with a high gas phase acidity and a weight of 140. No likely candidates were found. The previous studies from the Heidelberg group (Frenzel and Arnold, 1994; Kiendler et al., 2000; Kiendler and Arnold, 2002b) have not reported this ion. We note that the JP-5 fuel contains proprietary additives which may account for the 139-amu ion.

5. Sulfuric acid concentration

Mass spectra such as the ones shown in Fig. 2 are often used to derive neutral concentrations of sulfur

containing species (Arnold et al., 1981, 1996, 1998; Curtius et al., 1998; Davis et al., 1998; Eisele and Tanner, 1993; Möhler and Arnold, 1992; Schlager and Arnold, 1987; Viggiano and Arnold, 1981, 1983). The chemistry of H_2SO_4 production was given in Section 1. The negative-ion chemistry in the engines is initiated by electron attachment to O_2 (Christophorou, 1984; Ferguson et al., 1979). While a slow process, the abundance of O_2 ensures that O_2^- is the primary negative ion. A series of steps involving the CO_2 , O_2 , O_3 , and NO_y rapidly produce NO_3^- ions (Ferguson et al., 1979; Viggiano and Arnold, 1995), which may be clustered. HSO_4^- ions are the result of a proton transfer reaction of NO_3^- with H_2SO_4 as well as similar reactions involving $\text{NO}_3^-(\text{HNO}_3)_n^-$ and $\text{NO}_3^-(\text{H}_2\text{O})_n^-$. The high-engine-power mass spectra, in which some of the NO_3^- precursor ion intensity survived passage through the exhaust stream, may be used with laboratory reaction rates (Viggiano et al., 1982, 1997) and reaction times to estimate the H_2SO_4 concentration. For the conditions of the present jet engine measurements, we estimate that the reaction rate constant for the NO_3^- reaction with H_2SO_4 is $1.8 \times 10^{-9} \text{ cm}^3 \text{ s}^{-1}$ and that for the $\text{NO}_3^-(\text{HNO}_3)$ reaction with H_2SO_4 is $1.5 \times 10^{-9} \text{ cm}^3 \text{ s}^{-1}$ at 600 K. A weighed average of these reaction rates was used here. The reaction time from the engine exhaust plane to the IMS orifice was determined from the exhaust velocity as measured with a pitot tube. The reaction time varied (see Table 1) from 8 ms at 100% maximum compressor rpm to 51 ms at idle, but we did not observe the NO_3^- -related precursor ion for reaction times beyond 16 ms (80% maximum rpm).

The mass spectra obtained at both 90% and 100% maximum rpm yielded an H_2SO_4 concentration of $3.0 \times 10^{11} \text{ cm}^{-3}$, corresponding to a mixing ratio of 23 parts per billion by volume (ppbv). Normalizing to NASA-LaRC measurements of the CO_2 mixing ratio in the exhaust, H_2SO_4 emission indices may be derived: 0.0059 g (H_2SO_4)/kg (fuel) at 100% maximum rpm and 0.0081 g (H_2SO_4)/kg (fuel) at 90% maximum rpm. With the engine operating at 80% maximum rpm, the analogous figures are $1.9 \times 10^{11} \text{ cm}^{-3}$, corresponding to a mixing ratio of 14 ppbv and an emission index of 0.0055 g (H_2SO_4)/kg (fuel). For comparison with these figures, if the fuel sulfur (810 ppm) were to be totally converted into elemental S, its emission index would be 0.81 g (S)/kg (fuel). Comparing EI(S) to that for H_2SO_4 , and accounting for the 32/98 mass ratio, we find that 0.2–0.3% of the fuel sulfur appears to be in the form of H_2SO_4 . This result is lower than deduced from previous measurements (for different engines) (Kiendler et al., 2000, 2002b; Curtius et al., 1998). This may be due to the short sampling time and high temperatures used in the present study, which may prevent total conversion of SO_3 into H_2SO_4 . There is evidence for gaseous SO_3 in the exhaust in that an ion at 177 amu [presumably

$\text{HSO}_4^-(\text{SO}_3)$ is observed in the high-engine-rpm spectra. H_2SO_4 is also observed as a cluster at 195 amu, $\text{HSO}_4^-(\text{H}_2\text{SO}_4)$. Attempts to use these ions to determine concentrations of the ligands resulted in numbers that are very small, indicating the clustering is thermodynamically and not kinetically controlled due to the high temperatures. In earlier measurements of jet engine exhaust, in a test cell and in flight, at different power levels, essentially all of the fuel sulfur appeared in the form of SO_2 within a 20% uncertainty, implying that S(VI) species—both in gas phase and aerosols—are minor constituents of the exhaust (Hunton et al., 2000).

The estimates given above are subject to some qualifications. (1) We are assuming that the reaction between the NO_3^- -related precursor ions with H_2SO_4 takes place only between the engine exhaust plane and the IMS orifice, i.e., that the gases in the 1.8-m long augmentor section of the engine are too hot to allow significant buildup of H_2SO_4 . (2) We are assuming that the H_2SO_4 concentration is constant from the exhaust plane to the IMS orifice. (3) We are assuming that there are no significant competing reactions between NO_3^- -related precursor ions and species other than H_2SO_4 , aside from H_2O and HNO_3 clustering. (4) We are assuming that the ion–ion recombination loss rate affects all of the negative ions equally (Arnold, 1980; Bates, 1982, 1985; Smith and Adams, 1982). (5) The laboratory ion–molecule rate constants were measured under low-pressure conditions rather than in atmospheric air (but should not have a large pressure dependence since they proceed at the collisional rate). (6) The laboratory rate constants were measured at temperatures ≤ 343 K (but show little temperature dependence). (7) The intensities of the surviving NO_3^- , $\text{NO}_3^-(\text{H}_2\text{O})$, and $\text{NO}_3^-(\text{HNO}_3)$ ions were quite small by the time the IMS orifice was reached. We feel that the assumptions listed are good ones, but the cumulative effect, taken together with the small NO_3^- signal levels, lead us to say that the H_2SO_4 concentrations derived here should be taken as uncertain at the factor-of-three level.

6. High-mass ions

Integral-mode mass spectra were also obtained. Integral-mode spectra count all ions with masses between 9/7 and 16 times the resolving-mode mass. Above 150 amu, the integral-mode spectra are smooth and slowly decrease, with no obvious ledges, consistent with the finding that there are no dominant mass peaks at high masses. A few small mass peaks were observed in this range. However, the integral-mode spectrum is more intense by a factor of at least 100 than any single resolved peak in this mass range, an indication that there is a wide distribution of peaks with low intensity.

Fig. 3 shows both types of mass spectra taken at 60% engine power. The most intense mass peak is almost two orders of magnitude smaller than the sum of the ions in the integral mode. The integral spectrum decreases very slowly, indicating that the ion signal is spread over many masses, with 16% of the ions having masses > 300 amu and 6% > 570 amu (corrected for the 9/7 factor). Table 2 gives the fraction of ions with masses > 300 and 570 amu for each engine power setting. The quantity of higher masses grows with decreasing power in both classes of ions with more 6% or more being heavier than 570 amu, for engine powers $\leq 70\%$.

In order to obtain the mass distribution, we have taken the derivative of the intensity I of the

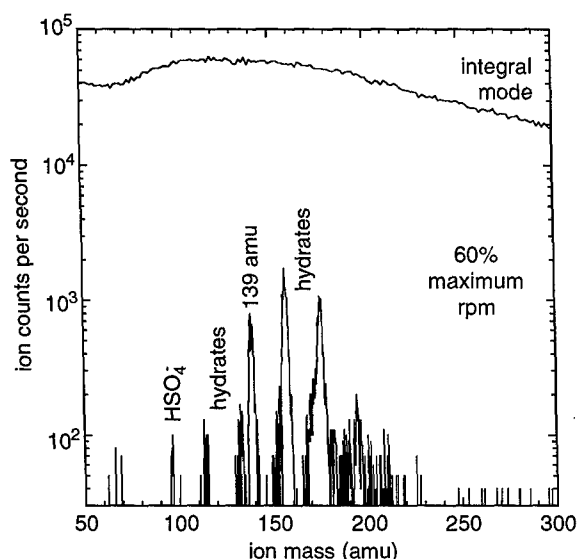


Fig. 3. Mass spectra obtained behind the J85 engine running at 60% power, in resolving- and integral-mode (“total-ion”) operation of the mass spectrometer. The integral-mode data have not been corrected for the 9/7 mass-scaling factor (see text).

Table 2

Fraction of chemiions with masses > 300 and 570 amu, sampled at 3.2 m behind the exhaust plane of the J85-GE-5H jet engine operating with JP-8 fuel containing 820 ppmv sulfur

Percent maximum rpm	Fraction of ions with masses > 300 amu	Fraction of ions with masses > 570 amu
100	0.014	0.005
90	0.05	0.009
80	0.12	0.030
70	0.15	0.059
60	0.16	0.061
50 (idle)	0.18	0.064

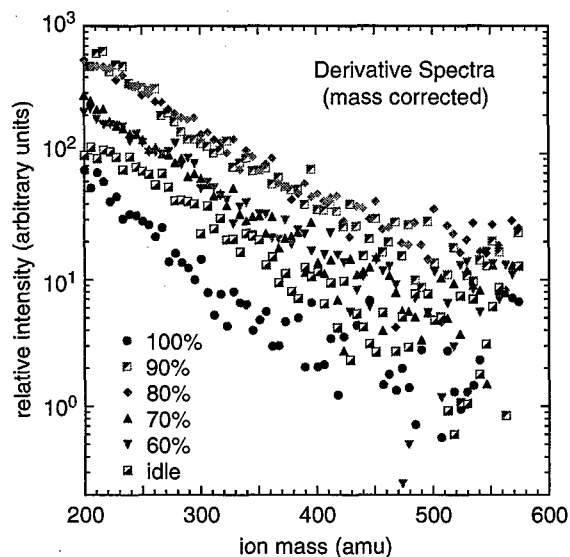


Fig. 4. Derivative of the total-ion spectra at each engine power setting. These plots are equivalent to mass spectra with very low resolution. The horizontal axis has been corrected for the 9/7 mass-scaling factor (see text).

integral-mode spectra with respect to mass m , i.e., $-dI/dm$. Since the ion intensity relates to all masses greater than the mass in question, the negative of the derivative is the ion intensity at that mass, although the resolution is poor. The data were smoothed before calculating $-dI/dm$. The results are shown in Fig. 4 for masses >200 amu. The 100% and 90% engine-power spectra show a peak near 100 amu (obviously HSO_4^-) with a width of about 10 amu, indicative of the low-resolution inherent with this technique. The data for all power settings decay approximately exponentially from 200 to about 450 amu. The higher masses appear to have a less-steep decay, indicating a broad distribution to very high masses. This feature would not be so obvious in the undifferentiated spectra because a constant ion distribution would there exhibit a linear decay with ion mass.

7. Ion concentration at the engine exit plane

The total-ion data in conjunction with laboratory calibrations may be used to estimate the ion concentration (plasma density) at the engine exhaust plane. The ion concentration at the IMS sampling orifice is much lower than at the engine plane because of ion-ion recombination reactions that take place in the exhaust stream; ion diffusion losses are much less important. The ion-ion recombination reaction rate constant is difficult to measure, especially for specific ion types. Bates (1985) has reviewed the problem, focusing on $\text{O}_4^+ + \text{O}_4^-$, and concluded that an effective two-body rate constant α of

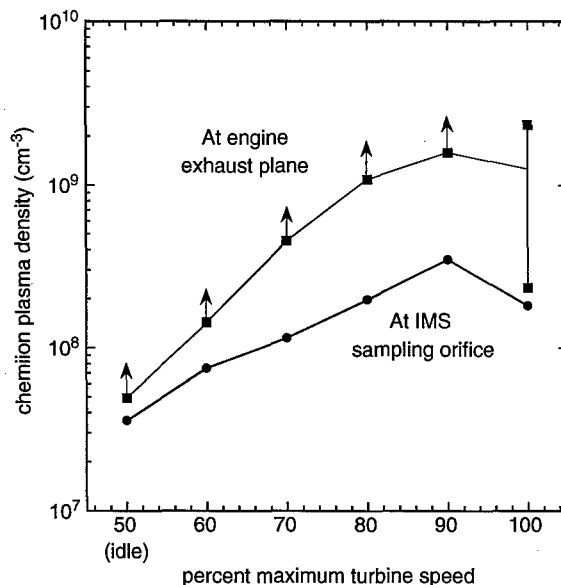


Fig. 5. The result of modeling backwards from the total IMS ion signal to obtain limits on the ion concentration at the exhaust plane of the T-38 jet engine. The ion loss in the sampling path is due to ion-ion recombination.

$1.6 \times 10^{-6} \text{ cm}^3 \text{ s}^{-1}$ is appropriate at 300 K and 1 atm, based on calculations and experiment. Temperature and pressure corrections lower the rate constant to about $5 \times 10^{-7} \text{ cm}^3 \text{ s}^{-1}$ for the conditions of the present data. Sorokin et al. (2002) have examined experimental and theoretical results for ion-ion recombination in flames. For the temperatures and pressures of the present work, they supply a lower limit to α in the range $1.5\text{--}2.5 \times 10^{-7} \text{ cm}^3 \text{ s}^{-1}$, and an upper limit in the range $6.1\text{--}9.5 \times 10^{-7} \text{ cm}^3 \text{ s}^{-1}$.

The concentration of negative ions at the engine exit is given as

$$[\text{exit}] = [\text{ims}] / (1 + [\text{ims}]\alpha\tau),$$

where $[\text{exit}]$ and $[\text{ims}]$ are the concentrations of negative ions at the exit plane and IMS, and τ is the reaction time. The recombination losses are so great for ion densities $\geq 10^9 \text{ cm}^{-3}$, that we neglect lesser losses such as ion diffusion or plume dilution. The concentration $[\text{ims}]$ is deduced from the laboratory determination of the IMS detection sensitivity discussed in Section 3. The results of the calculations are shown in Fig. 5. Values of α greater than about $5 \times 10^{-7} \text{ cm}^3 \text{ s}^{-1}$ lead to infinite ion densities at the engine, except for the 100%-power datum. Since α is not well known and the values of α are close to the limiting value, this procedure is highly uncertain. The lower values of α result in reasonable lower-limit values of plasma density at the engine exit plane. Increasing engine power generally shows that more ions exit the engine. However, the ion concentration at 100%

maximum rpm is lower than that at 90%. This seems counterintuitive and may be due to a systematic error in the 100% rpm datum, or, more likely, may imply that α is higher for the low-mass ions observed here at 100% engine power. The latter explanation is reasonable because at high pressures, α is determined by the mobilities of the positive and negative ions drifting toward each other, and the mobilities increase for lower-mass ions. Several of the data lie low enough that diffusion and dilution corrections were considered. At 350 K and 1 atm pressure, these corrections amounted to 1% for the 1-m distance behind the engine exhaust plane and the worst-case reaction time of 51 ms. The present lower limits to the ion concentration at the engine exhaust plane are of the same order as those found previously in both jet and car engine exhaust (Arnold et al., 2000; Yu et al., 2004). These are large enough that ion-induced nucleation is a likely source of volatile aerosols (Yu and Turco, 1997, 1998, 1999).

The lower limits to the ion concentrations at the engine exhaust plane may be combined with the NASA-LaRC CO₂ measurements to yield lower limits to emission indices for negative ions. These range from a low of $2 \times 10^{13} \text{ kg}^{-1}$ fuel at engine idle to a peak value of $5 \times 10^{15} \text{ kg}^{-1}$ fuel at 90% power.

8. Discussion

The group at the Max Planck Institute in Heidelberg has pioneered ion measurements in engine exhaust at the ground, in flight, and in combustors. The present measurements show both similarities and differences with those measurements. Here, we compare the present results to those made previously.

At least at higher engine power, the present measurements show ions with smaller masses than observed in the Heidelberg work, which we attribute both to the present shorter sampling times and higher sampling temperatures. The exception is the most recent unresolved data taken 2 ms after the combustor (Haverkamp et al., 2004). Higher temperatures lead to less solvation of ions since cluster bonds are weak (Keece and Castleman, 1986). In addition, the shorter sampling times and the high temperatures limit formation of H₂SO₄ and HNO₃ (Miake-Lye et al., 1993), which are key clustering agents.

The presence of large amounts of HSO₄⁻ core ions had been observed previously and was expected (Kiendler et al., 2000; Kiendler and Arnold, 2002b). In contrast, the finding of ions with 139-amu cores was not expected and is unexplained. The evolution with increasing reaction time (decreasing engine power) indicates that these ions are formed from HSO₄⁻ core ions in a reaction with a neutral species that has a high electron affinity or acidity. However, there are no obvious candidates

except speculations about proprietary compounds in JP-5 that might produce this unknown species after combustion. Its abundance would only need to be similar to that of H₂SO₄ or slightly smaller, if the rate of reaction is collisional.

The presence of high-mass ions has been observed previously (Arnold et al., 1999; Eichkorn et al., 2002; Haverkamp et al., 2004; Wohlfrom et al., 2000). In fact, the Heidelberg group found ions heavier than 8000 amu in flight. This latter measurement took place in the upper troposphere at a distance up to 1 km or 6.2 s behind an ATTAS test aircraft (Arnold et al., 1999). Those ions are considerably heavier than the ones observed in the present work, indicating that ion evolution continues for a considerably distance or time from leaving the engine. The large particles were interpreted as extending into the nanometer range (Wohlfrom et al., 2000). At the other end of the spectrum, the Heidelberg group has recently made ion mobility measurements in the exhaust of a combustor (Haverkamp et al., 2004). The reaction time was 2 ms after leaving the combustor and the temperature was 900–1000 K. These measurements were made with a low pass filter, i.e., the opposite of the integral-mode spectra reported here. In this case, the ions were relatively light, with half the ions having masses <40 amu. This should correspond to the primary ion, O₂⁻ (Viggiano and Arnold, 1995), although that was not hypothesized by the authors. The Heidelberg group also has a measurement taken 400 ms after the combustor, with most of that time in the sampling tube (Eichkorn et al., 2002).

The three data sets from the Heidelberg group can be combined with the present measurements to span plume ages from 2 ms up to several seconds. Fig. 6 shows a plot of the mass at which 50%, 25%, 10%, and 1% of the ions are heavier, vs. time. For the flight data we took an average plume age of 3 s, somewhat arbitrarily since the individual plume ages (0.6–6.2 s) for the data were not reported. The graph clearly shows the particles growing with time, mostly monotonically, in spite of the fact that the data refer to different conditions, e.g., altitude, engine model, fuel sulfur, and operating power. The mass at which 50% of the ions are heavier varies from 40 amu at 2 ms to 8000 amu at 3 s and the trend is monotonic despite the varying conditions. A similar trend is observed for the mass where 25% of the ions are heavier. Note that for the in-flight data we extrapolated slightly to get the ion mass since the published mass spectra never reduced to 25% of the maximum ion intensity. The 10% data are not completely monotonic, since the combustor results already show heavy ions. For only a few conditions could the mass for which 1% of the ions are heavier be derived. The masses from the present experiments are similar to the 10% point in the combustor experiment but considerably smaller than that found at 400 ms. The 3-s data imply more massive

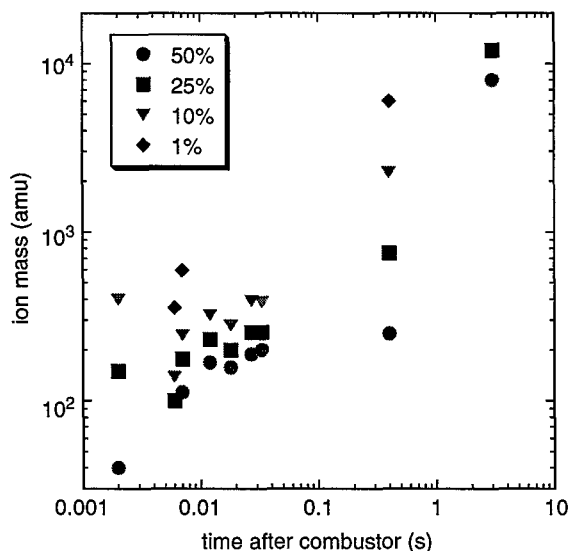


Fig. 6. Mass at which 50%, 25%, 10%, and 1% of the ions in the exhaust plume are heavier, for different experimental results with different jet engines and fuels.

ions than expected from the trends at lower plume ages. This may be due to the lower atmospheric temperature (~ 200 K) encountered during that portion of that flight, as one would expect low temperatures to promote clustering. The growth could be nonlinear with time since it is a multistep process and the rate-determining step may be early in the ion evolution. Positive-ion spectra also show very heavy ions (Eichkorn et al., 2002).

In a study involving only resolving-mode data after 400 ms plume age, the presence of clusters of the type $\text{HSO}_4^-(\text{H}_2\text{SO}_4)_n$ was unambiguously identified (Kiendler and Arnold, 2002b). Including the present results (which exhibit a considerable amount of hydration), the data show that growth occurs in large part by H_2O and H_2SO_4 addition as expected from a mechanism involving ion-induced nucleation (Lovejoy et al., 2004). Positive-ion mass spectra show the presence of numerous organic compounds (Kiendler and Arnold, 2002a). The presence of organic negative ions has also been observed but in low abundance (Kiendler et al., 2000).

Attention has recently been focused on ion-induced nucleation as a growth mechanism for volatile particles in engine exhaust (Kärcher et al., 1998; Yu and Turco, 1997, 1998, 1999; Yu et al., 1999). This process involves ion formation by chemiionization followed by solvation and coagulation. Ion–ion association to form bound ion pairs has also been postulated to be important (Arnold, 1980; Moseley et al., 1975; Turco et al., 1998). In any case, one expects ion growth to occur, and the data in Fig. 6 lend support to that mechanism. The measurements at the earliest times indicate that bare ions are present, perhaps O_2^- (the most likely ion with mass

<40 amu) in the combustor data and HSO_4^- in the present data at 100% and 90% power. The present data combined with results from earlier work show an evolution from bare ions, to hydrated ions, to ions with masses >8000 amu. The in-flight measurements found ions so massive that they should be thought as charged particulates, i.e., the nucleation had already occurred. The rest of the measurements show this evolution occurring to some extent. The size of the particles has been shown to be a function of fuel sulfur content, which presumably means a more direct function of sulfuric acid in the exhaust. This is not surprising since sulfuric acid readily condenses on ions in the presence of water.

9. Conclusions

The present results in combination with previous measurements show that ion-induced nucleation is a likely source of volatile aerosols in jet engine exhaust. The combined data set shows a time evolution of ions from unclustered ions to simple solvated species and finally to ions that can be considered to be small charged aerosols. The ion densities derived here are large enough that ion nucleation can be expected to be significant. Since only lower limits to the ion density at the engine exhaust plane could be estimated (and an upper limit for 100% power, where the sampling time was only 8 ms), the present experiment cannot offer a direct comparison between ion density for comparison with aerosol densities (Kärcher et al., 1998). However, the upper limit determined at full engine power lies far below the level of aerosol densities, so it seems clear that ions can induce nucleation of only a small fraction of aerosols, possibly those of one type or of one size distribution. Sulfuric acid concentrations determined in this work are lower than previous measurements made at longer reaction times, possibly reflecting incomplete conversion of SO_3 into H_2SO_4 by the time of our sampling.

Acknowledgements

The financial support of the NASA Atmospheric Effects of Aviation Project, the Air Force Office of Scientific Research, the Air Force Research Laboratory, and the Strategic Environmental Research and Development Program is gratefully acknowledged.

References

- Arnold, F., 1980. Multi-ion complexes in the stratosphere—implications for trace gases and aerosol. *Nature* 284, 610–611.

- Arnold, F., Fabian, R., Joos, W., 1981. Measurements of the height variation of sulfuric acid vapor concentrations in the stratosphere. *Geophysical Research Letters* 8, 293–296.
- Arnold, F., Wohlfrom, K.H., Klemm, M., Schneider, J., Gollinger, K., Schumann, U., Busen, R., 1996. Gaseous ion-composition measurements in the young exhaust plume of jet aircraft at cruising altitudes: implications for aerosols and gaseous sulfuric acid. Impact of Aircraft upon the Atmosphere, Paris.
- Arnold, F., Wohlfrom, K.-H., Klemm, M.W., Schneider, J., Gollinger, K., Schumann, U., Busen, R., 1998. First gaseous ion composition measurements in the exhaust plume of a jet aircraft in flight: implications for gaseous sulfuric acid, aerosols, and chemiions. *Geophysical Research Letters* 25, 2137–2140.
- Arnold, F., Curtius, J., Sierau, B., Burger, V., Busen, R., Schumann, U., 1999. Detection of massive negative chemiions in the exhaust plume of a jet aircraft in flight. *Geophysical Research Letters* 26, 1577–1580.
- Arnold, F., Kiendler, A., Wiedemer, V., Aberle, S., Stilp, T., Busen, R., 2000. Chemion concentration measurements in jet engine exhaust at the ground: implications for ion chemistry and aerosol formation in the wake of a jet engine. *Geophysical Research Letters* 27, 1723–1726.
- Ballenthin, J.O., Thorn, W.F., Miller, T.M., Viggiano, A.A., Hunton, D.E., Koike, M., Kondo, Y., Takegawa, N., Irie, H., Ikeda, H., 2003. In situ HNO_3 to NO_y instrument comparison during solve. *Journal of Geophysical Research* 108, ACH7-1–7-1.
- Bates, D.R., 1982. Recombination of small ions in the troposphere and lower stratosphere. *Planetary and Space Science* 30, 1275–1282.
- Bates, D.R., 1985. Ion-ion recombination in an ambient gas. *Advances in Atomic and Molecular Physics* 20, 1–40.
- Christophorou, L.G., 1984. In: Christophorou, L.G. (Ed.), *Electron-Molecule Interactions and Their Applications*. Academic, New York, pp. 477–617.
- Curtius, J., Sierau, B., Arnold, F., Baumann, R., Busen, R., Schulte, P., Schumann, U., 1998. First direct sulfuric acid detection in the exhaust plume of a jet aircraft in flight. *Geophysical Research Letters* 25, 923–926.
- Davis, D., Chen, G., Kasibhatla, P., Jefferson, A., Tanner, D., Eisele, F., Lenschow, D., Neff, W., Berresheim, H., 1998. DMS oxidation in the Antarctic marine boundary layer: comparison of model simulations and field observations of DMS, DMSO , DMSO_2 , $\text{H}_2\text{SO}_4(\text{g})$, $\text{MSA}(\text{g})$, and $\text{MSA}(\text{p})$. *Journal of Geophysical Research* 103, 1657–1678.
- Eichkorn, S., Wohlfrom, K.-H., Arnold, F., Busen, R., 2002. Massive positive and negative chemiions in the exhaust of an aircraft jet engine at ground level: mass distribution measurements and implications for aerosol formation. *Atmospheric Environment* 36, 1821–1825.
- Eisele, F.L., Tanner, D.J., 1993. Measurement of gas phase concentration of H_2SO_4 and MSA and estimates of H_2SO_4 production and loss in the atmosphere. *Journal of Geophysical Research* 98, 9001.
- Ferguson, E.E., Fehsenfeld, F.C., Albritton, D.L., 1979. In: Bowers, M.T. (Ed.), *Gas Phase Ion Chemistry*. Academic, San Diego, pp. 45–82.
- Frenzel, A., Arnold, F., 1994. Sulfuric acid cluster ion formation by jet engines: implications for sulfur acid formation and nucleation. In: Schumann, U., Wurzel, D. (Eds.), *Impact of Emissions from Aircraft and Spacecraft upon the Atmosphere*. DLR-Mitteilung 94-06, Deutsches Zentrum für Luft- und Raumfahrt, Oberpfaffenhofen and Cologne, Germany, pp. 106–112.
- Haverkamp, H., Wilhelm, S., Sorokin, A., Arnold, F., 2004. Positive and negative ion measurements in jet aircraft engine exhaust: concentrations, sizes, and implications for aerosol formation. *Atmospheric Environment* 38, 2879–2884.
- Hunton, D.E., Ballenthin, J.O., Borghetti, J.F., Federico, G.S., Miller, T.M., Thorn, W.F., Viggiano, A.A., Anderson, B.E., Cofer, W.R., McDougal, D.S., Wey, C.C., 2000. Chemical ionization mass spectrometric measurements of SO_2 emissions from jet engines in flight and test chamber operations. *Journal of Geophysical Research* 105, 26,841–26,855.
- Jayne, J.T., Poschl, U., Chen, Y.-M., Dai, D., Molina, L.T., Worsnop, D.R., Kolb, C.E., Molina, M.J., 1997. Pressure and temperature dependence of the gas-phase reaction of SO_3 with H_2O and the heterogeneous reaction of SO_3 and $\text{H}_2\text{O}/\text{H}_2\text{SO}_4$ surfaces. *Journal of Physical Chemistry* 101, 10,000–10,011.
- Kärcher, B., Yu, F., Schröder, F.P., Turco, R.P., 1998. Ultrafine aerosol particles in aircraft plumes: analysis of growth mechanisms. *Geophysical Research Letters* 25, 2793–2796.
- Keese, R.G., Castleman Jr., A.W., 1986. Thermochemical data on gas-phase ion-molecule association and clustering reactions. *Journal of Physical and Chemical Reference Data* 15, 1011.
- Kiendler, A., Arnold, F., 2002a. First composition measurements of positive chemiions in aircraft jet engine exhaust: detection of numerous ion species containing organic compounds. *Atmospheric Environment* 36, 2979–2984.
- Kiendler, A., Arnold, F., 2002b. Unambiguous identification and measurement of sulfuric acid cluster chemiions in aircraft engine exhaust. *Atmospheric Environment* 36, 1757–1761.
- Kiendler, A., Aberle, S., Arnold, F., 2000. Negative chemiions formed in jet fuel combustion: new insights from jet engine and laboratory measurements using a quadrupole ion trap mass spectrometer apparatus. *Atmospheric Environment* 34, 2623–2632.
- Kolb, C.E., Jayne, J.T., Worsnop, D.R., Molina, M.J., Meads, R.F., Viggiano, A.A., 1994. Gas phase reaction of sulfur trioxide with water vapor. *Journal of the American Chemical Society* 116, 10,314–10,315.
- Lovejoy, E.R., Hanson, D.R., Huey, L.G., 1996. Kinetics and products of the gas-phase reaction of SO_3 with water. *Journal of Physical Chemistry* 100, 19,911–19,916.
- Lovejoy, E.R., Curtius, J., Froyd, K.D., 2004. Atmospheric ion-induced nucleation of sulfuric acid and water. *Journal of Geophysical Research* 109.
- Mallard, W.G., Linstrom, P.J. (Eds.), 2001. *NIST Chemistry WebBook*. NIST Standard Reference Database No. 69, National Institutes of Standards and Technology, Gaithersburg, MD.
- Miake-Lye, R.C., Martinez-Sanchez, M., Brown, R.C., Kolb, C.E., 1993. Plume and wake dynamics, mixing, and chemistry behind a high speed civil transport. *Journal of Aircraft* 30, 467–479.

- Miller, T.M., Ballenthin, J.O., Meads, R.F., Hunton, D.E., Thorn, W.F., Viggiano, A.A., Kondo, Y., Koike, M., Zhao, Y., 2000. CIMS technique for the measurement of HNO_3 in air traffic corridors in the upper troposphere during the SONEX campaign. *Journal of Geophysical Research* 105, 3701–3707.
- Möhler, O., Arnold, F., 1992. Gaseous sulfuric acid and sulfur dioxide measurements in the arctic troposphere and lower stratosphere: implications for hydroxyl radical abundances. *Geophysical Research Letters* 17, 1763.
- Moseley, J.T., Olson, R.E., Peterson, J.R., 1975. Ion–ion mutual neutralization. *Case Studies in Atomic Physics* 5, 1–45.
- Reiner, T., Arnold, F., 1994. Laboratory investigations of gaseous sulfuric acid formation via $\text{SO}_3 + \text{H}_2\text{O} + \text{M} \rightarrow \text{H}_2\text{SO}_4 + \text{M}$: measurements of rate constant and product identification. *Journal of Chemical Physics* 101, 7399–7407.
- Schlager, H., Arnold, F., 1987. Balloon-borne composition measurements of stratospheric negative ions and inferred sulfuric acid vapor abundances during the map/globus 1983 campaign. *Planetary and Space Science* 35, 693–701.
- Smith, D., Adams, N.G., 1982. Ionic recombination in the stratosphere. *Geophysical Research Letters* 9, 1085–1087.
- Sorokin, A., Vancassel, X., Mirabel, P., 2002. Emission of ions and charged soot particles by aircraft engines. *Atmospheric Chemistry and Physical Discussion* 2, 2045–2074.
- Sorokin, A., Arnold, F., Mirabel, P., 2003. On the influence of fuel sulfur induced stable negative ion formation on the total concentration of ions emitted by an aircraft gas turbine engine: comparison of model and experiment. *Atmospheric Chemistry and Physical Discussion* 3, 6001–6018.
- Turco, R.P., Zhao, J., Yu, F., 1998. A new source of tropospheric aerosols: ion–ion recombination. *Geophysical Research Letters* 25, 635–638.
- Viggiano, A.A., Arnold, F., 1981. Extended sulfuric acid concentration measurements in the stratosphere. *Geophysical Research Letters* 8, 583.
- Viggiano, A.A., Arnold, F., 1983. Stratospheric sulfuric acid vapor—new and updated results. *Journal of Geophysical Research* 88, 1457.
- Viggiano, A.A., Arnold, F., 1995. In: Volland, H. (Ed.), *Atmospheric Electrodynamics*. CRC Press, Boca Raton, FL, pp. 1–25.
- Viggiano, A.A., Perry, R.A., Albritton, D.L., Ferguson, E.E., Fehsenfeld, F.C., 1980. The role of H_2SO_4 in stratospheric negative-ion chemistry. *Journal of Geophysical Research* 85, 4551.
- Viggiano, A.A., Perry, R.A., Albritton, D.L., Ferguson, E.E., Fehsenfeld, F.C., 1982. Stratospheric negative-ion reaction rates with H_2SO_4 . *Journal of Geophysical Research* 87, 7340–7342.
- Viggiano, A.A., Henchman, M.J., Dale, F., Deakynne, C.A., Paulson, J.F., 1992. Gas-phase reactions of weak bronsted bases I^- , PO_3^- , HSO_4^- , FSO_3^- , and CF_3SO_3^- with strong bronsted acids H_2SO_4 , FSO_3H , and $\text{CF}_3\text{SO}_3\text{H}$. A quantitative intrinsic superacidity scale for the sulfonic acids XSO_3H ($\text{X} = \text{HO}$, F , and CF_3). *Journal of the American Chemical Society* 114, 4299.
- Viggiano, A.A., Seeley, J.V., Mundis, P.L., Williamson, J.S., Morris, R.A., 1997. Rate constants for the reactions of $\text{XO}_3(\text{H}_2\text{O})_n$ ($\text{X} = \text{C}$, HC , and N) and $\text{NO}_3(\text{HNO}_3)_n$ with H_2SO_4 : implications for atmospheric detection of H_2SO_4 . *Journal of Physical Chemistry A* 101, 8275.
- Wang, X.B., Nicholas, J.B., Wang, L.S., 2000. Photoelectron spectroscopy and theoretical calculations of SO_4^- and HSO_4^- : confirmation of high electron affinities of SO_4 and HSO_4 . *Journal of Physical Chemistry A* 104, 504–508.
- Wohlfrom, K.-H., Eichkorn, S., Arnold, F., 2000. Massive positive and negative ions in the wake of a jet aircraft: detection by a novel aircraft-based large ion mass spectrometer (LIOMAS). *Geophysical Research Letters* 27, 3853–3856.
- Yu, F., Turco, R.P., 1999. Evolution of aircraft-generated volatile particles in the far wake regime: potential contributions to ambient CCN/IN. *Geophysical Research Letters* 26, 1703–1706.
- Yu, F., Turco, R.P., 1997. The role of ions in the formation and evolution of particles in aircraft plumes. *Geophysical Research Letters* 24, 1927–1930.
- Yu, F., Turco, R.P., 1998. Contrail formation and impacts on aerosol properties in aircraft plumes: effects of fuel sulfur content. *Geophysical Research Letters* 25, 313–316.
- Yu, F., Turco, R.P., Kärcher, B., 1999. The possible role of organics in the formation and evolution of ultrafine aircraft particles. *Journal of Geophysical Research* 104, 4079–4087.
- Yu, F., Lanni, T., Frank, B.P., 2004. Measurements of ion concentration in gasoline and diesel engine exhaust. *Atmospheric Environment* 38, 1417–1423.